Mechanics of Composite Materials and Structures, 7:153–175, 2000

1075-9417/00 $12.00 + .00

Transverse Stress Decay in a Specially Orthotropic Strip under Localized Normal Edge Loading

W. B. FICHTER

NASA Langley Research Center, Hampton, Virginia, USA

ABSTRACT

Solutions are presented for the stresses in a specially orthotropic infinite strip which is subjected to localized uniform normal loading on one edge while the other edge is either restrained against normal displacement only, or completely fixed. The solutions are used to investigate the diffusion of load into the strip and in particular the decay of normal stress across the width of the strip. For orthotropic strips representative of a broad range of balanced and symmetric angle-ply composite laminates, minimum strip widths are found that ensure at least 90% decay of the normal stress across the strip. In addition, in a few cases where, on the fixed edge the peak shear stress exceeds the normal stress in magnitude, minimum strip widths that ensure 90% decay of both stresses are found.

To help in putting these results into perspective, and to illustrate the influence of material properties on load diffusion in orthotropic materials, closed-form solutions for the stresses in similarly loaded orthotropic half-planes are obtained. These solutions are used to generate illustrative stress contour plots for several representative laminates. Among the laminates, those composed of intermediate-angle plies, i.e., from about 30° to 60°, exhibit marked changes in normal stress contour shape with stress level.

The stress contours are also used to find 90% decay distances in the half-planes. In all cases, the minimum strip widths for 90% decay of the normal stress exceed the 90% decay distances in the corresponding half-planes, in amounts ranging from only a few percent to about 50% of the half-plane decay distances. The 90% decay distances depend on both material properties and the boundary conditions on the supported edge.

The widespread and growing use of composite materials in recent years has prompted increased interest in analysis of the stresses and deformations in elastic anisotropic materials. As a result, it is well known that stress decay rates in anisotropic elastic bodies can differ markedly from those in similarly loaded isotropic bodies. (See, for example, [1] and [2], where numerous studies are cited.) Many of the cited studies have focused on questions concerning the applicability of St. Venant's principle to anisotropic bodies, particularly elastic strips that are loaded in the longitudinal direction. One finding of such investigations is that the distance over which end effects in axially loaded anisotropic strips diffuse and decay to insignificant levels can differ by an order of magnitude or more from that in an isotropic strip, a result which has obvious implications in the determination of elastic properties of composite materials from laboratory tests of small specimens. In [3], solutions were found for the stresses in a specially orthotropic half-plane subjected to localized

Address correspondence to W. B. Fichter, 113 Pierce's Court, Williamsburg, VA 23185, USA. E-mail: wbfichter@erols.com

NOMENCLATURE

A, B, C, D	coefficients in solution to transformed governing equation	u, v	in-plane displacements
		x, y	rectangular Cartesian coordinates
E_x, E_y, G_{xy}, η_{xy}, η_{yx}	elastic constants for orthotropic materials	y_d	90% decay distance for σ_y in the half-plane
h	dimensionless width of strip	γ	characteristic root of transformed governing equation
h_d	minimum strip width required to ensure 90% decay of σ_y	$\varepsilon_x, \varepsilon_y, \tau_{xy}$	elastic strains
		λ	Fourier transformation variable
k, k_1, k_2, q, r	characteristic parameters	$\sigma_x, \sigma_y, \tau_{xy}$	elastic stresses
p	magnitude of applied normal traction	$\varphi(x, y)$	Airy stress function

Subscripts C and S indicate Fourier sine and cosine transforms, respectively.

self-equilibrated edge loading, and a simple approximate formula was found for a lower bound on the normalized 90% decay distance for the normal stress.

There are practical concerns as well for the decay of stresses *across the width* of elastic strips. Many modern aircraft and spacecraft structural components are laminated composite panels which, for many purposes of structural analysis, can be modeled as orthotropic strips. It is of interest to designers of such components to know, for example, how loads applied to one edge of an orthotropic strip are reacted at the other edge or, more specifically, how wide a particular strip must be to ensure that the reaction stresses at all points on the supported edge are no more than a specified fraction of the applied loads.

Making this type of information available to designers is the primary purpose of this article. A specially orthotropic (principal axes of orthotropy aligned with coordinate axes) elastic strip is subjected to localized uniform normal loading on one edge, while the opposite edge is either restrained against normal displacement only, or completely fixed. For both edge-support modes, expressions are found for the stresses at all points in the strip. Extensive numerical results for the stresses along the opposite edge of the strip are presented for a broad range of symmetric angle-ply laminates. To aid in putting these results in perspective, solutions are also presented for the similarly loaded and supported isotropic strip and the similarly loaded specially orthotropic and isotropic half-planes.

ANALYSIS

The specially orthotropic strip studied here is defined by $-\infty < x < \infty$, $0 \le y \le h$. The engineering constants are E_x, E_y, G_{xy}, η_{xy}, and η_{yx}, where $E_x \nu_{yx} = E_y \nu_{xy}$. For plane stress conditions the stresses, strains, and displacements are related by

$$\varepsilon_x = u_{,x} = \frac{\sigma_x}{E_x} - \eta_{yx}\frac{\sigma_y}{E_y} \qquad \varepsilon_y = \eta_{,y} = \frac{\sigma_y}{E_y} - \mu_{xy}\frac{\sigma_x}{E_x}$$
$$\gamma_{xy} = \eta_{,y} + v_{,x} = \frac{\tau_{xy}}{G_{xy}} \tag{1}$$

The stresses are defined in terms of the Airy stress function by

$$\sigma_x = \varphi_{,yy} \qquad \sigma_y = \varphi_{,xx} \qquad \tau_{xy} = -\varphi_{,xy} \tag{2}$$

where the comma followed by a subscript indicates partial differentiation with respect to the subscript variable. Thus, the plane-stress equilibrium equations are satisfied automatically, and the compatibility equation can be written as

$$\frac{E_x}{E_y}\varphi_{,xxxx} + \left(\frac{E_x}{G_{xy}} - 2\eta_{xy}\right)\varphi_{,xxyy} + \varphi_{,yyyy} = 0 \tag{3}$$

Two boundary-value problems for the specially orthotropic strip, referred to herein as problems A and B, are analyzed here. In both problems, uniform normal traction of magnitude p is applied to the free edge $y = 0$ over an interval of length 2, which, for simplicity, is centered on the y axis. (Note that the stresses in all the solutions presented here can be easily converted to solutions for applied traction over an interval of length $2a$ by substituting x/a and y/a for x and y.) In problem A, the edge $y = h$ is partially fixed, i.e., the shear stress τ_{xy} and normal displacement v are set equal to zero. In problem B, the edge $y = h$ is completely fixed, i.e., both the normal and tangential displacements, u and v, are set equal to zero. The solution to problem A is presented first.

Problem A—Partially fixed upper edge

The boundary conditions are

$$\tau_{xy}(x, 0) = 0 \tag{4}$$

$$\sigma_y(x, 0) = \begin{cases} p & |x| \le 1 \\ 0 & |x| \ge 1 \end{cases} \tag{5}$$

$$\tau_{xy}(x, h) = 0 \tag{6}$$

$$v(x, h) = 0 \tag{7}$$

The unbounded domain and the discontinuous edge loading suggest a Fourier transform approach. The Fourier cosine and sine transforms are defined by

$$\varphi_C(\lambda, y) = \sqrt{\frac{2}{\pi}} \int_0^\infty \varphi(x, y) \cos \lambda x \, dx \qquad \text{or}$$
$$\varphi_S(\lambda, y) = \sqrt{\frac{2}{\pi}} \int_0^\infty \varphi(x, y) \sin \lambda x \, dx \tag{8}$$

and inversely,

$$\varphi(x, y) = \sqrt{\frac{2}{\pi}} \int_0^\infty \varphi_C(\lambda, y) \cos \lambda x \, d\lambda \qquad \text{or}$$
$$\varphi(x, y) = \sqrt{\frac{2}{\pi}} \int_0^\infty \varphi_S(\lambda, y) \sin \lambda x \, d\lambda \tag{9}$$

In terms of the transformed stress function, the transformed stresses and displacements are

$$\sigma_{xC} = \varphi_{C,yy} \qquad \sigma_{yC} = -\lambda^2\varphi_C \qquad \tau_{xyS} = \lambda\varphi_{C,y}$$
$$u_S = \left(\frac{1}{\lambda E_x}\right)\varphi_{C,yy} + \left(\frac{\eta_{yx}}{E_y}\right)\lambda\varphi_C \qquad \text{and} \tag{10}$$
$$v_C = \left(\frac{1}{\lambda^2 E_x}\right)\varphi_{C,yyy} + \left(\frac{\eta_{yx}}{E_y} - \frac{1}{G_{xy}}\right)\varphi_{C,y}$$

which anticipate obvious symmetries about the y axis in both problems. Application of the appropriate transforms to the governing equations yields

$$\varphi_{C,yyyy} - \left(\frac{E_x}{G_{xy}} - 2\eta_{xy}\right)\lambda^2\varphi_{C,yy} + \left(\frac{E_x}{E_y}\right)\lambda^4\varphi_C = 0 \tag{11}$$

along with

$$\varphi_{C,y}(\lambda, 0) = 0 \tag{12}$$

$$\varphi_C(\lambda, 0) = -p\sqrt{\frac{2}{\pi}}\left(\frac{\sin\lambda}{\lambda^3}\right) \equiv -f(\lambda) \tag{13}$$

$$\varphi_{C,y}(\lambda, h) = 0 \tag{14}$$

and

$$\varphi_{C,yyy}(\lambda, h) - \left(\frac{E_x}{G_{xy}} - \nu_{xy}\right)\lambda^2\varphi_{C,y}(\lambda, h) = 0$$

which in view of Eq. (14) simplifies to

$$\varphi_{C,yyy}(\lambda, h) = 0 \tag{15}$$

When the solution to Eq. (11) is assumed to have the form $\varphi_C = F(\lambda)e^{\lambda\gamma y}$, the following characteristic equation is obtained:

$$\gamma^4 - \left(\frac{E_x}{G_{xy}} - 2\eta_{xy}\right)\gamma^2 + \left(\frac{E_x}{E_y}\right) = 0 \tag{16}$$

With the definitions $2r = (E_x/G_{xy} - 2\eta_{xy})$, $k^4 = E_x/E_y$, Eq. (16) becomes

$$\gamma^4 - 2r\gamma^2 + k^4 = 0 \tag{17}$$

The form of the solution for $\varphi_C(\lambda, y)$ depends on the nature of the characteristic roots, which depends on the material constants through the parameters r and k, as seen in Eq. (17). With the physically meaningless special cases disregarded, the three material

types of engineering interest are:

Type I: $0 < k^2 < r$. Let $q = \sqrt{r^2 - E_x/E_y}$, and $k_1 = \sqrt{r+q}$, $k_2 = \sqrt{r-q}$. Then $\gamma = \pm k_1, \pm k_2$ (real, distinct).

Type II: $0 < k^2 = r$. Then $\gamma = \pm k, \pm k$ (real, repeated).

Type III: $0 < |r| < k^2$. Let $k_1 = \sqrt{(k^2+r)/2}$, $k_2 = \sqrt{(k^2-r)/2}$. Then $\gamma = \pm(k_1 \pm ik_2)$ (equal and opposite conjugate pairs).

Most balanced and symmetric angle-ply laminates are of type I or type III. However, one type II material of great practical interest is the isotropic (or quasi-isotropic) material. The isotropic solution can be found from a type I or type III solution through an appropriate limiting process, as well as by dealing directly with the isotropic formulation.

Solution for type I material

The transformed stress function has the form

$$\varphi_C(\lambda, y) = A(\lambda)\cosh\lambda k_1 y + B(\lambda)\sinh\lambda k_1 y + C(\lambda)\cosh\lambda k_2 y + D(\lambda)\sinh\lambda k_2 y \quad (18)$$

Substitution of Eq. (18) into the transformed boundary conditions, Eqs. (12)–(15), leads to simultaneous algebraic equations to be solved for A, B, C, and D, which are then substituted into Eq. (18) to completely define $\varphi_C(\lambda, y)$. Then the use of Eqs. (8)–(10) gives for the stresses at any point in the strip,

$$\sigma_x = (2p/\pi)k_1k_2\int_0^\infty [k_1\sinh\lambda k_2 h\cosh\lambda k_1(h-y) - k_2\sinh\lambda k_1 h\cosh\lambda k_2(h-y)]\sin\lambda\cos\lambda x\, d\lambda/\Delta \quad (19)$$

$$\sigma_y = (2p/\pi)\int_0^\infty [k_1\sinh\lambda k_1 h\cosh\lambda k_2(h-y) - k_2\sinh\lambda k_2 h\cosh\lambda k_1(h-y)]\sin\lambda\cos\lambda x\, d\lambda/\Delta \quad (20)$$

$$\tau_{xy} = (2p/\pi)k_1k_2\int_0^\infty [\sinh\lambda k_1 h\sinh\lambda k_2(h-y) - \sinh\lambda k_2 h\sinh\lambda k_1(h-y)]\sin\lambda\sin\lambda x\, d\lambda/\Delta \quad (21)$$

where

$$\Delta = \lambda(k_1\sinh\lambda k_1 h\cosh\lambda k_2 h - k_2\cosh\lambda k_1 h\sinh\lambda k_2 h) \quad (22)$$

On the supported edge $y = h$, the nonzero stresses are

$$\sigma_x(x, h) = 2(k_1^2 + k_2^2)p/\pi\int_0^\infty [k_1\sinh\lambda k_2 h - k_2\sinh\lambda k_1 h]\sin\lambda\cos\lambda x\, d\lambda/\Delta \quad (23)$$

$$\sigma_y(x, h) = (2p/\pi)\int_0^\infty [k_1\sinh\lambda k_1 h - k_2\sinh\lambda k_2 h]\sin\lambda\cos\lambda x\, d\lambda/\lambda\Delta \quad (24)$$

Solution for type III material

With the characteristic-value definitions $\gamma = k_1 + ik_2$ and $\bar{\gamma} = k_1 - ik_2$ for type III materials, the transformed stress function has the form

$$\varphi_C(\lambda, y) = A(\lambda)\cosh\lambda\gamma y + B(\lambda)\sinh\lambda\gamma y + C(\lambda)\cosh\lambda\bar{\gamma} y + D(\lambda)\sinh\lambda\bar{\gamma} y \quad (25)$$

Satisfaction of the transformed boundary conditions, Eqs. (12)–(15), and the subsequent use of Eqs. (25) and (8)–(10), yields the following expressions for the stresses at any point in the strip:

$$\sigma_x = 2p(k_1^2 + k_2^2)/\pi \int_0^\infty [F_1 \cosh \lambda k_1(h - y) \cos \lambda k_2(h - y) + F_2 \sinh \lambda k_1(h - y) \sin \lambda k_2(h - y)] \sin \lambda \cos \lambda x \, d\lambda/\Delta \tag{26}$$

where

$$F_1 = k_2 \sinh \lambda k_1 h \cos \lambda k_2 h - k_1 \cosh \lambda k_1 h \sin \lambda k_2 h$$

$$F_2 = k_2 \cosh \lambda k_1 h \sin \lambda k_2 h + k_1 \sinh \lambda k_1 h \cos \lambda k_2 h$$

$$\sigma_y = 2p/\pi \int_0^\infty \{k_2[\sinh \lambda k_1 h \cos \lambda k_2 y \cosh \lambda k_1(h - y) - \sin \lambda k_2 h \sinh \lambda k_1 y \sin \lambda k_2(h - y)] + k_1[\sin \lambda k_2 h \cosh \lambda k_1 y \cos \lambda k_2(h - y) + \sinh \lambda k_1 h \sin \lambda k_2 y \sinh \lambda k_1(h - y)]\} \sin \lambda \cos \lambda x \, d\lambda/\Delta \tag{27}$$

$$\tau_{xy} = 2p(k_1^2 + k_2^2)/\pi \int_0^\infty [\sinh \lambda k_1 h \sin \lambda k_2 y \cosh \lambda k_1(h - y) - \sin \lambda k_2 h \sinh \lambda k_1 y \cos \lambda k_2(h - y)] \sin \lambda \sin \lambda x \, d\lambda/\Delta \tag{28}$$

where

$$\Delta = \lambda(k_2 \sinh \lambda k_1 h \cosh \lambda k_1 h + k_1 \sin \lambda k_2 h \cos \lambda k_2 h) \tag{29}$$

On the supported edge $y = h$, the nonzero stresses are

$$\sigma_x(x, h) = 2p(k_1^2 + k_2^2)/\pi \int_0^\infty [k_2 \sinh \lambda k_1 h \cos \lambda k_2 h - k_1 \cosh \lambda k_1 h \sin \lambda k_2 h] \sin \lambda \cos \lambda x \, d\lambda/\Delta \tag{30}$$

$$\sigma_y(x, h) = 2p/\pi \int_0^\infty [k_2 \sinh \lambda k_1 h \cos \lambda k_2 h + k_1 \cosh \lambda k_1 h \sin \lambda k_2 h] \sin \lambda \cos \lambda x \, d\lambda/\Delta \tag{31}$$

Solution for isotropic material

The details of the solution are presented in the Appendix. The formulas for the stresses at any point in the strip are

$$\sigma_x = 2p/\pi \int_0^\infty [\sinh \lambda y + \sinh \lambda(2h - y) - \lambda(2h - y) \cosh \lambda y - \lambda y \cosh \lambda(2h - y)] \sin \lambda \cos \lambda x \, d\lambda/\Delta \tag{32}$$

$$\sigma_y = 2p/\pi \int_0^\infty [\sinh \lambda y + \sinh \lambda(2h - y) + \lambda(2h - y) \cosh \lambda y + \lambda y \cosh \lambda(2h - y)] \sin \lambda \cos \lambda x \, d\lambda/\Delta \tag{33}$$

$$\tau_{xy} = 2p/\pi \int_0^\infty [\lambda y \sinh \lambda(2h - y) - \lambda(2h - y) \sinh \lambda y] \sin \lambda \sin \lambda x \, d\lambda/\Delta \tag{34}$$

where

$$\Delta = \lambda(\sinh 2\lambda h + 2\lambda h) \tag{35}$$

On the supported edge $y = h$, the nonzero stresses are

$$\sigma_x(y, h) = 4p/\pi \int_0^\infty [\sinh \lambda h - \lambda h \cosh \lambda h] \sin \lambda \cos \lambda x \, d\lambda/\Delta \tag{36}$$

$$\sigma_y(x, h) = 4p/\pi \int_0^\infty [\sinh \lambda h + \lambda h \cosh \lambda h] \sin \lambda \cos \lambda x \, d\lambda/\Delta \tag{37}$$

Problem B—Fixed upper edge

The boundary conditions are

$$\tau_{xy}(x, 0) = 0 \tag{38}$$

$$\sigma_y(x, 0) = \begin{Bmatrix} p & |x| \le 1 \\ 0 & |x| > 1 \end{Bmatrix} \tag{39}$$

$$u(x, h) = 0 \tag{40}$$

and

$$v(x, h) = 0 \tag{41}$$

In terms of φ_C, the transformed boundary conditions are

$$\varphi_{C,y}(\lambda, 0) = 0 \tag{42}$$

$$\varphi_C(\lambda, 0) = -p\sqrt{\frac{2}{\pi}}\left(\frac{\sin \lambda}{\lambda^3}\right) \equiv -f(\lambda) \tag{43}$$

$$\varphi_{C,yy}(\lambda, h) + \lambda^2 \eta_{xy} \varphi_C(\lambda, h) = 0 \tag{44}$$

and

$$\varphi_{C,yyy}(\lambda, h) + \lambda^2\left(\eta_{xy} - \frac{E_x}{G_{xy}}\right)\varphi_{C,y}(\lambda, h) = 0 \tag{45}$$

Solution for type I material

The use of Eq. (18) in conjunction with Eqs. (42)–(45) yields a set of simultaneous equations which is solved for A, B, C, and D. These are used along with Eqs. (18) and (8)–(10) to obtain the expressions for the stresses at any point in the strip:

$$\begin{aligned}\sigma_x = 2pk_1k_2/\pi \int_0^\infty \{&(\xi^2 - \eta^2)(k_1^2 \cosh \lambda k_1 y + k_2^2 \cosh \lambda k_2 y) \\ &+ (\xi + \eta)^2[k_1k_2 \sinh \lambda k_2 h \sinh \lambda k_1(h - y) - k_2^2 \cosh \lambda k_1 h \cosh \lambda k_2(h - y)] \\ &+ (\xi - \eta)^2[k_1k_2 \sinh \lambda k_1 h \sinh \lambda k_2(h - y) - k_1^2 \cosh \lambda k_2 h \cosh \lambda k_1(h - y)]\} \\ &\sin \lambda \cos \lambda x \, d\lambda/\Delta\end{aligned} \tag{46}$$

$$\sigma_y = 2p/\pi \int_0^\infty \{k_1k_2[(\xi-\eta)^2 \cosh \lambda k_2 h \cosh \lambda k_1(h-y) + (\xi+\eta)^2 \cosh \lambda k_1 h \cosh \lambda k_2(h-y) - (\varepsilon-\eta)(\cosh \lambda k_1 y + \cosh \lambda k_2 y)] - k_1^2(\varepsilon-\eta)^2 \sinh \lambda k_1 h \sinh \lambda k_2(h-y) - k_2^2(\xi+\eta)^2 \sinh \lambda k_2 h \sinh \lambda k_1(h-y)\} \times \sin \lambda \cos \lambda x \, d\lambda/\Delta \quad (47)$$

$$\tau_{xy} = 2pk_1k_2/\pi \int_0^\infty \{(\xi^2-\eta^2)(k_1 \sinh \lambda k_1 y + k_2 \sinh \lambda k_2 y) + k_1(\xi-\eta)^2[\cosh \lambda k_2 h \sinh \lambda k_1(h-y) - \sinh \lambda k_1 h \cosh \lambda k_2(h-y)] + k_2(\xi+\eta)^2[\cosh \lambda k_1 h \sinh \lambda k_2(h-y) - \sinh \lambda k_2 h \cosh \lambda k_1(h-y)]\} \sin \lambda \sin \lambda x \, d\lambda/\Delta \quad (48)$$

where

$$\xi = 1/2(k_1^2 + k_2^2 + 2v_{xy}) \qquad \eta = 1/2(k_1^2 - k_2^2) \quad (49)$$

$$\Delta = \lambda\{2k_1k_2[(\xi^2+\eta^2)\cosh \lambda k_1 h \cosh \lambda k_2 h - (\xi^2-\eta^2)] - [k_1^2(\xi-\eta)^2 + k_2^2(\xi+\eta)^2] \sinh \lambda k_1 h \sinh \lambda k_2 h\} \quad (50)$$

Along the fixed edge $y = h$, the formulas simplify to

$$\sigma_x(x, h) = \eta_{xy}\sigma_y(x, h) \text{ (as required by the fixed-edge condition)} \quad (51)$$

$$\sigma_y(x, h) = 4pk_1k_2\eta/\pi \int_0^\infty [(\xi+\eta)\cosh \lambda k_1 h - (\xi-\eta)\cosh \lambda k_2 h] \sin \lambda \cos \lambda x \, d\lambda/\Delta \quad (52)$$

$$\tau_{xy}(x, h) = 4pk_1k_2\eta/\pi \int_0^\infty [k_1(\xi-\eta)\sinh \lambda k_1 h - k_2(\xi+\eta)\sinh \lambda k_2 h] \sin \lambda \sin \lambda x \, d\lambda/\Delta \quad (53)$$

Solution for type III material

Substitution of Eq. (25) into the transformed boundary conditions (42)–(45) produces a set of simultaneous equations which are solved for A, B, C, and D. Substitution of their values into Eq. (25) and subsequent use of Eqs. (8)–(10) yields for the stresses,

$$\sigma_x = 2\gamma\bar{\gamma}p/\pi \int_0^\infty \mathrm{Re}[g\bar{g}\gamma^2 \cosh \lambda\gamma y + \gamma\bar{\gamma}g^2 \sinh \lambda\bar{\gamma}h \sinh \lambda\gamma(h-y) - \gamma^2\bar{g}^2 \cosh \lambda\bar{\gamma}h \cosh \lambda\gamma(h-y)] \sin \lambda \cos \lambda x \, d\lambda/\tilde{\Delta} \quad (54)$$

$$\sigma_y = 2p/\pi \int_0^\infty \mathrm{Re}[\gamma\bar{\gamma}g^2 \cosh \lambda\gamma h \cosh \lambda\bar{\gamma}(h-y) - g\bar{g}\cosh \lambda\gamma y - \gamma^2\bar{g}^2 \sinh \lambda\gamma h \sinh \lambda\bar{\gamma}(h-y)] \sin \lambda \cos \lambda x \, d\lambda/\tilde{\Delta} \quad (55)$$

$$\tau_{xy} = 2\gamma\bar{\gamma}p/\pi \int_0^\infty \mathrm{Re}[\gamma\bar{g}^2 \cosh \lambda\bar{\gamma}h \sinh \lambda\gamma(h-y) + \gamma g\bar{g} \sinh \lambda\gamma y - \gamma\bar{g}^2 \sinh \lambda\gamma h \cosh \lambda\bar{\gamma}(h-y)] \sin \lambda \sin \lambda x \, d\lambda/\tilde{\Delta} \quad (56)$$

where again $\gamma = k_1 + ik_2$, $\bar{\gamma} = k_1 - ik_2$, and $g = \gamma^2 + \eta_{xy}$, $\bar{g} = \bar{\gamma}^2 + v_{xy}$.

$\mathrm{Re}\{z\}$ indicates the real part of the complex number z, and

$$\tilde{\Delta} = \lambda\{\gamma\bar{\gamma}[\mathrm{Re}(g^2)\cosh\lambda\gamma h\cosh\lambda\bar{\gamma}h - g\bar{g}] - \mathrm{Re}(\bar{\gamma}^2 g^2)\sinh\lambda\gamma h\sinh\lambda\bar{\gamma}h\}$$

or, in explicitly real terms,

$$\begin{aligned}\tilde{\Delta} = \lambda\big(&\big(k_1^2+k_2^2\big)\big[4k_1^2k_2^2 - \big(k_1^2-k_2^2+\eta_{xy}\big)^2\big](\sinh^2\lambda k_1 h + \cos^2\lambda k_2 h)\\ &+\big(k_1^2+k_2^2\big)\big[\big(k_1^2-k_2^2+\eta_{xy}\big)^2 + 4k_1^2k_2^2\big] + \big\{\big(k_1^2-k_2^2\big)\big[\big(k_1^2-k_2^2+\eta_{xy}\big)^2 - 4k_1^2k_2^2\big]\\ &+8k_1^2k_2^2\big(k_1^2-k_2^2+\eta_{xy}\big)\big\}(\sinh^2\lambda k_1 h + \sin^2\lambda k_2 h)\big)\end{aligned} \tag{57}$$

On the fixed edge $y = h$, the expressions for the stresses become

$$\sigma_x(x,h) = \eta_{xy}\sigma_y(x,h) \text{ (as required by the fixed-edge condition)} \tag{58}$$

$$\begin{aligned}\sigma_y(x,h) = 8k_1k_2\big(k_1^2+k_2^2\big)p/\pi\int_0^\infty &[2k_1k_2\cosh\lambda k_1 h\cos\lambda k_2 h\\ &+\big(k_1^2-k_2^2+\eta_{xy}\big)\sinh\lambda k_1 h\sin\lambda k_2 h]\sin\lambda\cos\lambda x\,d\lambda/\tilde{\Delta}\end{aligned} \tag{59}$$

and

$$\begin{aligned}\tau_{xy}(x,h) = 8k_1k_2\big(k_1^2+k_2^2\big)p/\pi\int_0^\infty &\big[k_1\big(k_1^2+k_2^2+\mu_{xy}\big)\cosh\lambda k_1 h\sin\lambda k_2 h\\ &-k_2\big(k_1^2+k_2^2-\mu_{xy}\big)\sinh\lambda k_1 h\cos\lambda k_2 h\big]\sin\lambda\sin\lambda x\,d\lambda/\tilde{\Delta}\end{aligned} \tag{60}$$

Solution for isotropic material

The details of the solution are presented in the Appendix. The formulas for the stresses at any point in the strip are

$$\begin{aligned}\sigma_x = 2p/\pi\int_0^\infty &\{(3-\nu)\sinh\lambda h[\sinh\lambda(h-y) - \lambda y\cosh\lambda(h-y)]\\ &+[4\eta/(1+\eta) - (1+\eta)\lambda^2 h(h-y)]\cosh\lambda y\\ &+[(1+\eta)\lambda h + 2\lambda y]\sinh\lambda y\}\sin\lambda\cos\lambda x\,d\lambda/\Delta\end{aligned} \tag{61}$$

$$\begin{aligned}\sigma_y = 2p/\pi\int_0^\infty &\{(3-\eta)\sinh\lambda h(\sinh\lambda(h-y) + \lambda y\cosh\lambda(h-y))\\ &+[(1+\eta)\lambda^2 h(h-y) + 4/(1+\eta)]\cosh\lambda y\\ &+[(1+\eta)\lambda h - 2\lambda y]\sinh\lambda y\}\sin\lambda\cos\lambda x\,d\lambda/\Delta\end{aligned} \tag{62}$$

$$\begin{aligned}\tau_{xy} = 2p/\pi\int_0^\infty &\{(3-\eta)\lambda y\sinh\lambda h\sinh\lambda(h-y) + 2\lambda y\cosh\lambda y\\ &-[2(1-\eta)/(1+\eta) + (1+\eta)\lambda^2 h(h-y)]\}\sin\lambda\sin\lambda x\,d\lambda/\Delta\end{aligned} \tag{63}$$

where

$$\Delta = \lambda[(3-\eta)\sinh^2\lambda h + (1+\eta)\lambda^2 h^2 + 4/(1+\eta)] \tag{64}$$

On the fixed edge $y = h$,

$$\sigma_x(x, h) = \eta\sigma_y(x, h) \text{ (as required by the fixed-edge condition)} \tag{65}$$

$$\sigma_y(x, h) = 2p/\pi \int_0^\infty [2\lambda h \sinh 2\lambda h + 4/(1+\eta)\cosh 2\lambda h] \sin\lambda \cos\lambda x \, d\lambda/\Delta \tag{66}$$

$$\tau_{xy}(x, h) = 4p/\pi \int_0^\infty [\lambda h \cosh \lambda h - (1-\eta)/(1+\eta)\sinh \lambda h] \sin\lambda \sin\lambda x \, d\lambda/\Delta \tag{67}$$

Half-plane solutions

The equations governing the behavior of the orthotropic half-plane are those for the corresponding strip, except that the conditions on the edge $y = h$ are replaced by the requirement that the stresses vanish for $x^2 + y^2 \to \infty$ in the upper half-plane. The Fourier sine and cosine transforms can again be usefully employed.

Solution for type I material

Because of the requirement that the stresses vanish for $x^2 + y^2 \to \infty$, Eq. (18) can be replaced by

$$\varphi_C(\lambda, y) = A(\lambda)\exp(-\lambda k_1 y) + B(\lambda)\exp(-\lambda k_2 y) \tag{68}$$

Satisfaction of the two transformed boundary conditions, Eqs. (12) and (13), leads to

$$\varphi_C(\lambda, y) = f(\lambda)/(k_1 - k_2)[k_2 \exp(-\lambda k_1 y) - k_1 \exp(-\lambda k_2 y)]$$

Then, the use of Eqs. (8)–(10) gives

$$\sigma_x = 2pk_1k_2/[\pi(k_1 - k_2)] \int_0^\infty [k_1 \exp(-\lambda k_1 y) - k_2 \exp(-\lambda k_2 y)] \sin\lambda \cos\lambda x \, d\lambda/\lambda$$

$$\sigma_y = 2p/[\pi(k_1 - k_2)] \int_0^\infty [k_1 \exp(-\lambda k_2 y) - k_2 \exp(-\lambda k_1 y)] \sin\lambda \cos\lambda x \, d\lambda/\lambda$$

$$\tau_{xy} = 2pk_1k_2/[\pi(k_1 - k_2)] \int_0^\infty [\exp(-\lambda k_2 y) - \exp(-\lambda k_1 y)] \sin\lambda \sin\lambda x \, d\lambda/\lambda$$

All integrals can be evaluated in closed form [4]. The results are

$$\begin{aligned}\sigma_x = {} & 2pk_1k_2/[\pi(k_1 - k_2)]\big(k_1\{1/2 \operatorname{Arctan}[2k_1 y/(k_1^2 y^2 + x^2 - 1)] + S_1\pi/2\} \\ & - k_2\{1/2 \operatorname{Arctan}[2k_2 y/(k_2^2 y^2 + x^2 - 1)] + S_2\pi/2\}\big)\end{aligned} \tag{69}$$

$$\begin{aligned}\sigma_y = {} & 2p/[\pi(k_1 - k_2)]\big(k_1\{1/2 \operatorname{Arctan}[2k_2 y/(k_2^2 y^2 + x^2 - 1)] + S_2\pi/2\} \\ & - k_2\{1/2 \operatorname{Arctan}[2k_1 y/(k_1^2 y^2 + x^2 - 1)] + S_1\pi/2\}\big)\end{aligned} \tag{70}$$

$$\begin{aligned}\tau_{xy} = {} & pk_1k_2/[2\pi(k_1 - k_2)]\big(\ln\{[k_2^2 y^2 + (x+1)^2]/[k_2^2 y^2 + (x-1)^2]\} \\ & - \ln\{[k_1^2 y^2 + (x+1)^2]/[k_1^2 y^2 + (x-1)^2]\}\big)\end{aligned} \tag{71}$$

where

$$S_1 = \begin{Bmatrix} 1 & k_1^2y^2 + x^2 - 1 < 0 \\ 0 & k_1^2y^2 + x^2 - 1 \geq 0 \end{Bmatrix} \quad \text{and} \quad S_2 = \begin{Bmatrix} 1 & k_2^2y^2 + x^2 - 1 < 0 \\ 0 & k_2^2y^2 + x^2 - 1 \geq 0 \end{Bmatrix} \tag{72}$$

and k_1 and k_2 are the type I characteristic values defined earlier.

Solution for type III material

For this material, after enforcement of the requirement that all stresses vanish for $x^2 + y^2 \to \infty$ in the upper half-plane, the transformed stress function takes the form

$$\varphi_C(\lambda, y) = A(\lambda)\exp[-\lambda(k_1 + ik_2)y] + B(\lambda)\exp[-\lambda(k_1 - ik_2)y] \tag{73}$$

Satisfaction of the two transformed boundary conditions yields

$$\varphi_C(\lambda, y) = -f(\lambda)\exp(-\lambda k_1 y)[\cos\lambda k_2 y + (k_1/k_2)\sin\lambda k_2 y] \tag{74}$$

Then the use of Eqs. (8)–(10) gives

$$\sigma_x = -2p\left(k_1^2 + k_2^2\right)/\pi \int_0^\infty [(k_1/k_2)\sin\lambda k_2 y - \cos\lambda k_2 y]\exp(-\lambda k_1 y)\sin\lambda\cos\lambda x\, d\lambda/\lambda$$

$$\sigma_y = 2p/\pi \int_0^\infty [(k_1/k_2)\sin\lambda k_2 y + \cos\lambda k_2 y]\exp(-\lambda k_1 y)\sin\lambda\cos\lambda x\, d\lambda/\lambda$$

$$\tau_{xy} = 2p\left(k_1^2 + k_2^2\right)/(\pi k_2) \int_0^\infty \exp(-\lambda k_1 y)\sin\lambda k_2 y\sin\lambda\sin\lambda x\, d\lambda/\lambda$$

Again, all integrals can be evaluated in closed form [4]. The results are

$$\begin{aligned}\sigma_x = {} & -p\left(k_1^2 + k_2^2\right)/\pi\big[(k_1/4k_2)\big(\ln\big\{\left[k_1^2y^2 + (1 + k_2y + x)^2\right]/\left[k_1^2y^2 + (1 - k_2y - x)^2\right]\big\} \\ & + \ln\big\{\left[k_1^2y^2 + (1 + k_2y - x)^2\right]/\left[k_1^2y^2 + (1 - k_2y + x)^2\right]\big\}\big) \\ & - 1/2\,\text{Arctan}\big\{2k_1y/\left[k_1^2y^2 - 1 + (k_2y + x)^2\right]\big\} - S_1\pi/2 \\ & - 1/2\,\text{Arctan}\big\{2k_1y/\left[k_1^2y^2 - 1 + (k_2y - x)^2\right]\big\} - S_2\pi/2\big]\end{aligned} \tag{75}$$

$$\begin{aligned}\sigma_y = {} & p/\pi\big[(k_1/4k_2)\big(\ln\big\{\left[k_1^2y^2 + (1 + k_2y + x)^2\right]/\left[k_1^2y^2 + (1 - k_2y - x)^2\right]\big\} \\ & + \ln\big\{\left[k_1^2y^2 + (1 + k_2y - x)^2\right]/\left[k_1^2y^2 + (1 - k_2y + x)^2\right]\big\}\big) \\ & + 1/2\,\text{Arctan}\big\{2k_1y/\left[k_1^2y^2 - 1 + (k_2y + x)^2\right]\big\} + S_1\pi/2 \\ & + 1/2\,\text{Arctan}\big\{2k_1y/\left[k_1^2y^2 - 1 + (k_2y - x)^2\right]\big\} + S_2\pi/2\big]\end{aligned} \tag{76}$$

where

$$S_1 = \begin{Bmatrix} 1 & k_1^2y^2 - 1 + (k_2y + x)^2 < 0 \\ 0 & k_1^2y^2 - 1 + (k_2y + x)^2 \geq 0 \end{Bmatrix} \qquad S_2 = \begin{Bmatrix} 1 & k_1^2y^2 - 1 + (k_2y - x)^2 < 0 \\ 0 & k_1^2y^2 - 1 + (k_2y - x)^2 \geq 0 \end{Bmatrix} \tag{77}$$

and

$$\begin{aligned}\tau_{xy} = {} & p\left(k_1^2 + k_2^2\right)/(2\pi k_2)\{\text{Arctan}[(k_2y + x - 1)/(k_1y)] + \text{Arctan}[(k_2y - x + 1)/(k_1y)] \\ & - \text{Arctan}[(k_2y + x + 1)/(k_1y)] - \text{Arctan}[(k_2y - x - 1)/(k_1y)]\}\end{aligned} \tag{78}$$

Solution for isotropic material

This solution is readily available in the literature [5]. The stresses are

$$\sigma_x = (p/\pi)\{\text{Arctan}[y/(x-1)] - \text{Arctan}[y/(x+1)] + 2y(x^2 - y^2 - 1)/[(x^2 + y^2 - 1)^2 + 4y^2]\} \quad (79)$$

$$\sigma_y = (p/\pi)\{\text{Arctan}[y/(x-1)] - \text{Arctan}[y/(x+1)] - 2y(x^2 - y^2 - 1)/[(x^2 + y^2 - 1)^2 + 4y^2]\} \quad (80)$$

$$\tau_{xy} = (p/\pi)\{4xy^2/[(x^2 + y^2 - 1)^2 + 4y^2]\} \quad (81)$$

where the Arctan functions have the range $[0, \pi]$.

Results and discussion

In order to generate illustrative numerical and graphical results for stresses in some specially orthotropic configurations, a standard laminate analysis routine was used to compute equivalent orthotropic-sheet properties for a wide variety of symmetric angle-ply laminates in which each graphite-epoxy lamina had the following properties: $E_L = 128$ GPa, $E_T = 11.0$ GPa, $\eta_{LT} = 0.35$, and $G_{LT} = 5.74$ GPa, where subscripts L and T denote longitudinal and transverse directions relative to the fibers. Table 1 contains a list of 20 balanced and symmetric 24-ply laminates along with their equivalent orthotropic properties, their corresponding characteristic values, and their designation as type I, type III, or the one quasi-isotropic type II. Ply angles are measured from the positive x axis.

Table 1

Elastic constants and characteristic values of various laminates (moduli given in GPa)

Laminate	$E_x(10^{-6})$	$E_y(10^{-6})$	η_{xy}	$G_{xy}(10^6)$	Type	k_1	k_2
$[0]_{24}$	128	11.0	0.350	5.74	I	4.58	0.742
$[\pm 5]_{6S}$	125	11.0	0.421	6.56	I	4.19	0.803
$[\pm 10]_{6S}$	118	11.1	0.617	8.96	I	3.31	0.983
$[\pm 15]_{6S}$	105	11.2	0.879	12.5	I	2.12	1.44
$[\pm 20]_{6S}$	86.9	11.4	1.11	17.0	III	1.45	0.813
$[\pm 25]_{6S}$	67.2	11.8	1.24	21.8	III	1.16	1.02
$[\pm 30]_{6S}$	49.4	12.5	1.21	26.3	III	0.924	1.06
$[\pm 35]_{6S}$	35.5	13.9	1.09	29.9	III	0.745	1.02
$[\pm 40]_{6S}$	26.0	16.1	0.913	32.3	III	0.616	0.944
$[\pm 45]_{6S}$	19.9	19.9	0.731	33.1	III	0.534	0.846
$[\pm 50]_{6S}$	16.1	26.0	0.565	32.3	III	0.485	0.743
$[\pm 55]_{6S}$	13.9	35.5	0.425	29.9	III	0.465	0.639
$[\pm 60]_{6S}$	12.5	49.4	0.309	26.3	III	0.467	0.536
$[\pm 65]_{6S}$	11.8	67.2	0.217	21.8	III	0.487	0.427
$[\pm 70]_{6S}$	11.4	86.9	0.146	17.0	III	0.525	0.294
$[\pm 75]_{6S}$	11.2	105	0.094	12.5	I	0.472	0.694
$[\pm 80]_{6S}$	11.1	118	0.058	8.96	I	0.302	1.02
$[\pm 85]_{6S}$	11.0	125	0.037	6.56	I	0.239	1.25
$[90]_{24}$	11.0	128	0.030	5.74	I	0.218	1.35
Isotropic	50.9	50.9	0.312	19.4	II	1	1

In the numerical computation of stresses from either improper integrals or closed-form solutions, and in the graphical representation of the results, extensive use was made of Mathematica™ software [6]. Since all of the improper integrals in problems A and B required numerical integration, considerable experimentation was performed to establish a practical upper limit in place of $\lambda = \infty$. An upper integration limit of $\lambda = 20$ was found to be more than sufficient in all cases examined.

The closed forms of the solutions to the orthotropic and isotropic half-plane problems make it convenient and, it is hoped, instructive to present some half-plane results in advance of results for the strips.

Half-plane constant-stress contours

To illustrate some of the effects that material properties can have on load diffusion rates and patterns, contour plots for the normalized stresses σ_y/p and τ_{xy}/p are presented in Figures 1 and 2, respectively, for the isotropic half-plane and for orthotropic half-planes which correspond to the following seven laminates: $[0]_{24}$, $[\pm 15]_{6S}$, $[\pm 30]_{6S}$, $[\pm 45]_{6S}$, $[\pm 60]_{6S}$, $[\pm 75]_{6S}$, and $[90]_{24}$. To aid in making direct comparisons, all plots have been generated for the same square region defined by $\{-6 < x < 6, 0 < y < 12\}$.

Figure 1, which contains the five level curves $\sigma_y/p = 0.9, 0.7, 0.5, 0.3$, and 0.1 for each of the eight laminates, shows clearly that diffusion of the external loading into the half-plane is strongly influenced by laminate properties. For example, the maximum depth (i.e., distance, normalized by the width of the loaded region, from the edge $y = 0$) at which σ_y/p persists at the 10% level varies from about 6 for the $[\pm 30]_{6S}$ laminate to very much more than 12 for the $[90]_{24}$ laminate. The corresponding depth for the isotropic laminate lies well within these extremes.

In addition, among the eight laminates there are large differences in the shapes of corresponding constant-σ_y/p contours, especially for the lower levels of σ_y/p. In fact, contours for the intermediate-ply-angle laminates, i.e., those composed of $\pm 30°$, $\pm 45°$, and $\pm 60°$ plies, exhibit a fundamental shape change as σ_y/p becomes small. For large values of σ_y/p the contours display an absolute maximum along the y axis, their axis of symmetry, whereas for small values of σ_y/p they develop a relative minimum there. This behavior is consistent with the fact that the intermediate-angle-ply laminates have preferred directions of load propagation that are oblique to the direction of loading (90°), a feature that is especially evident in the $[\pm 45]_{6S}$ laminate (Figure 1*e*).

Before contour plots of normalized shear stress, τ_{xy}/p, for the eight laminates were generated, ranges for τ_{xy}/p had to be established. This was done by examining the limiting behavior of τ_{xy} in the neighborhood of $(x, y) = (1, 0)$, a point of discontinuity of the edge loading, where the shear stress has an extreme value. For $\tau_{\max} = \lim_{y \to 0} \tau_{xy}(1, y)$, the following expressions were obtained:

$$\tau_{\max}/p = \begin{cases} \dfrac{k_1 k_2}{\pi(k_1 - k_2)} \log \dfrac{k_1}{k_1} & \text{(type I)} \\ \dfrac{k_1^2 + k_2^2}{\pi k_2} \operatorname{Arctan} \dfrac{k_2}{k_1} & \text{(type III)} \\ \dfrac{1}{\pi} & \text{(isotropic)} \end{cases}$$

Upon appropriate passage to the limit, the type I and type III expressions reduce to the isotropic result. Numerical values of the maximum shear stresses in the eight featured

laminates are as follows:

Laminate	τ_{max}/p
Isotropic	0.318
$[0]_{24}$	0.513
$[\pm 15]_{6S}$	0.553
$[\pm 30]_{6S}$	0.507
$[\pm 45]_{6S}$	0.379
$[\pm 60]_{6S}$	0.256
$[\pm 75]_{6S}$	0.181
$[90]_{24}$	0.151

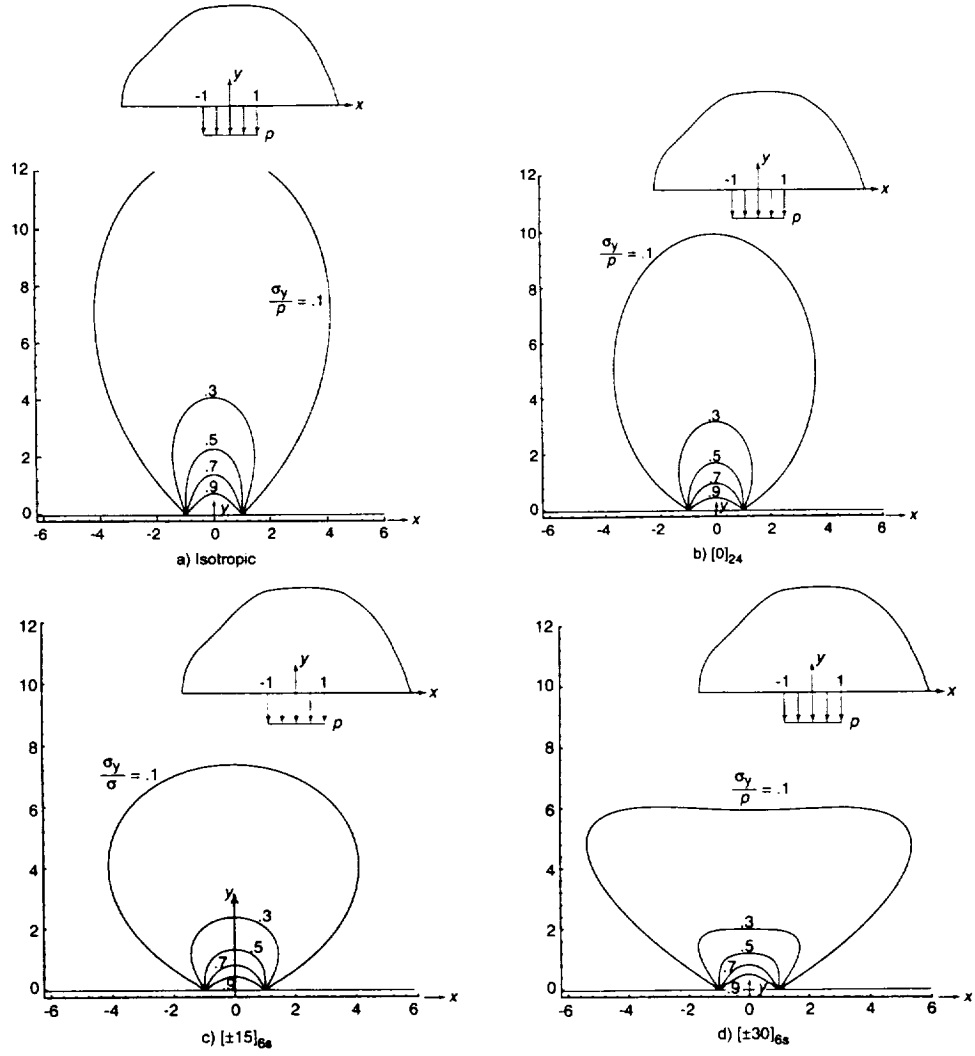

Figure 1. *Constant-σ_y plots for eight different laminates. (Continued)*

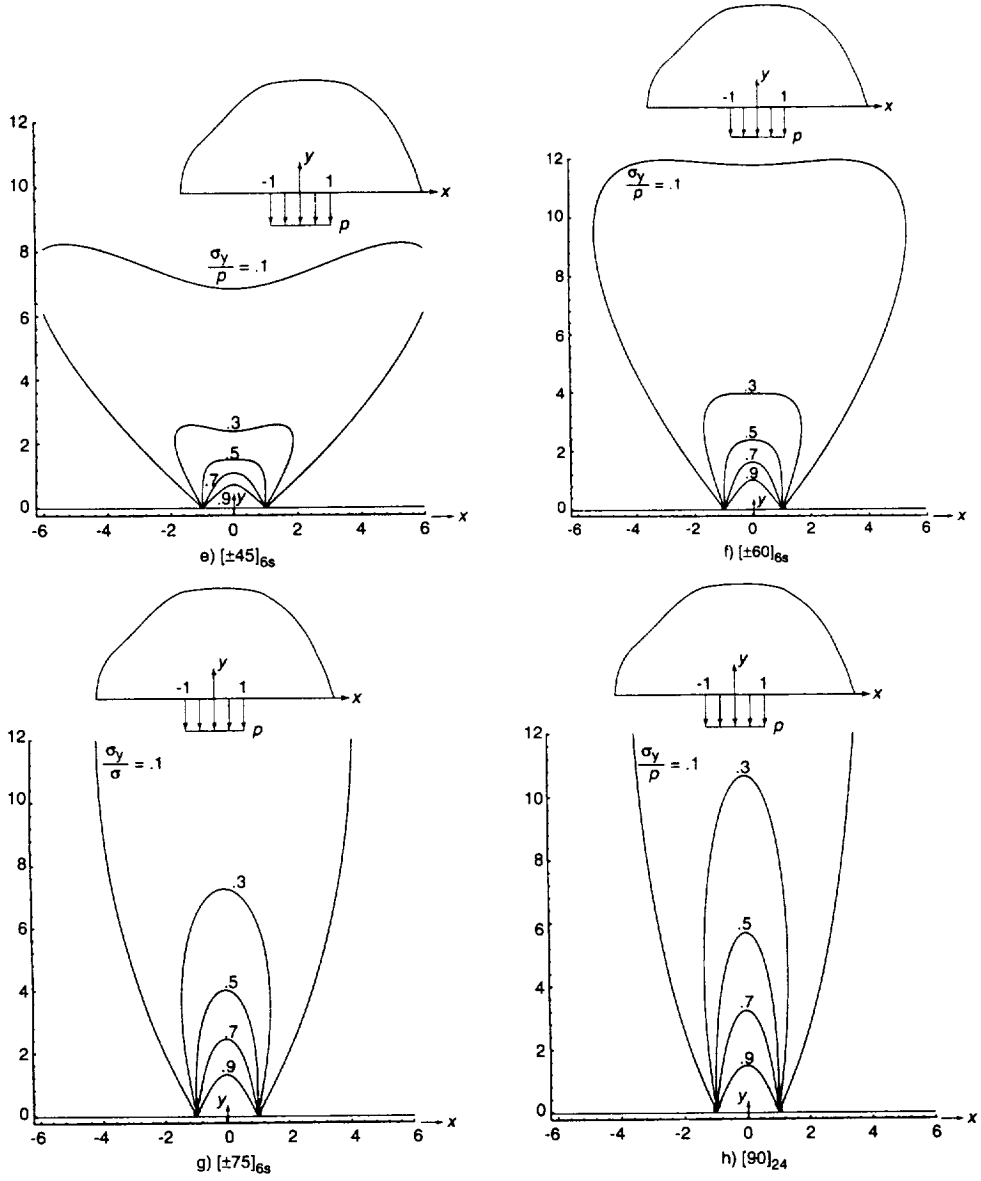

Figure 1. *Constant-σ_y plots for eight different laminates. (Continued).*

In Figure 2, level curves are shown for $\tau_{xy}/p = \pm 0.05$ and for equal increments of ± 0.05 to the $\{^{\text{maximum}}_{\text{minimum}}\}$ value, for which a level curve for τ_{xy}/p could be generated. Hence, the number of curves shown for a laminate is indicative of the severity of the shear stress field in that laminate. Also, there is positive correlation between the severity of the shear stress field and the rate of decay of the direct stress due to the normal loading. For example, in the $[\pm 15]_{6S}$ laminate the high shear stresses (Figure 2*c*) are consistent with the highly compact σ_y field (Figure 1*c*). Similarly, in the $[90]_{24}$ laminate the benign shear stress field (Figure 2*h*) correlates with the gradual decay of σ_y (Figure 1*h*).

These stress contour plots for the half-plane have been presented for two reasons. First the relatively simple closed-form solutions for the half-plane lend themselves to economical

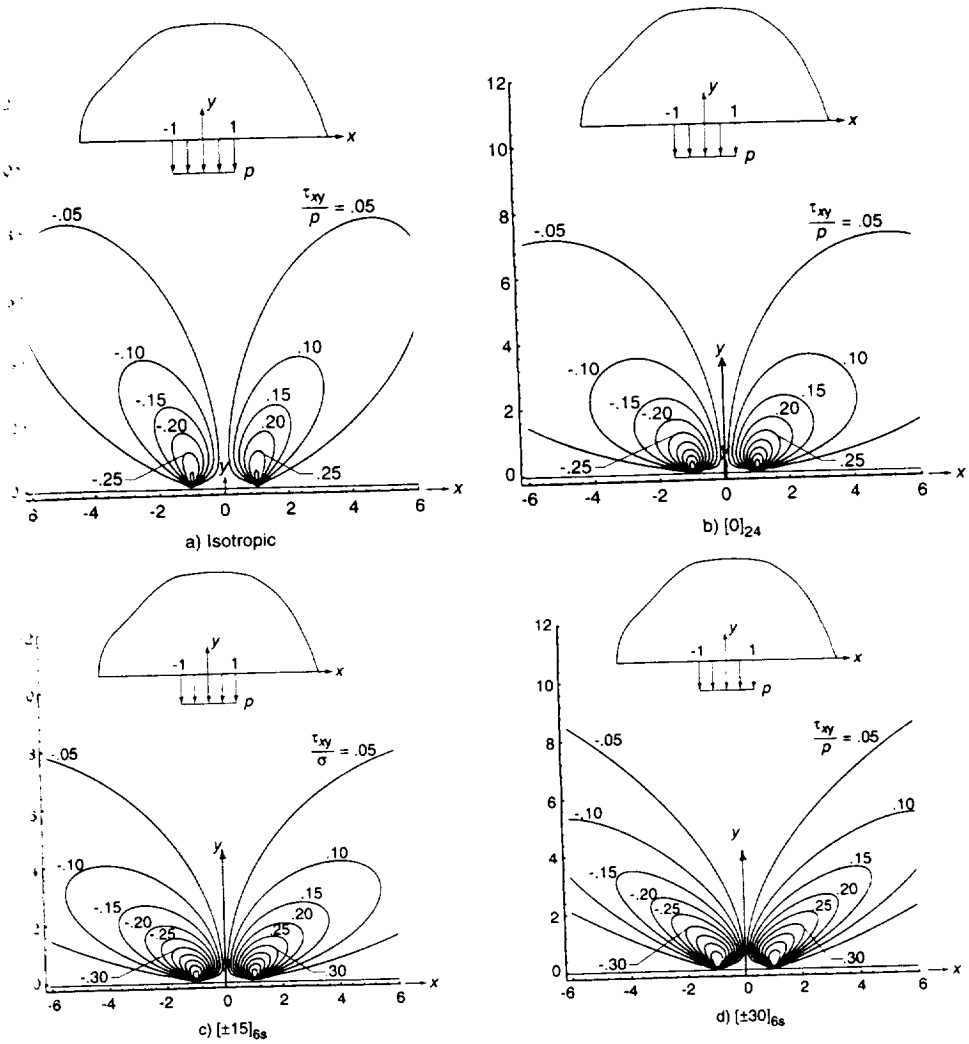

Figure 2. *Constant-τ_{xy} plots for eight different laminates. (Continued)*

contour-plot generation, while the strip solutions, in their somewhat involved improper integral forms, do not. Second, although the stress contour plots for the half-plane cannot be expected to mirror exactly the behavior of the elastic strips, the results may be helpful in visualizing the corresponding responses of the strips, if proper account can be taken of effects of the support conditions along the edge $y = h$. Information from the half-plane solutions that might be useful in this regard is y_d, the 90% decay distance for σ_y, which is defined here as the minimum (normalized) distance from the loaded edge for which $\sigma_y(x, y_d)/p \leq 0.1$ for all x.

To find y_d for most of the laminates, it sufficed to examine σ_y only along the y axis because every level curve for σ_y has a maximum there. However, as was noted earlier, for the $[\pm 30]_{6S}$ and $[\pm 60]_{6S}$ laminates, and presumably for all balanced angle-ply laminates between these, the level curves $\sigma_y/p = 0.1$ exhibit a relative minimum on the y axis. Thus, for those laminates the $\sigma_y/p = 0.1$ level curves had to be examined further to find the correct value of y_d. For the 20 laminates studied here, the values of y_d

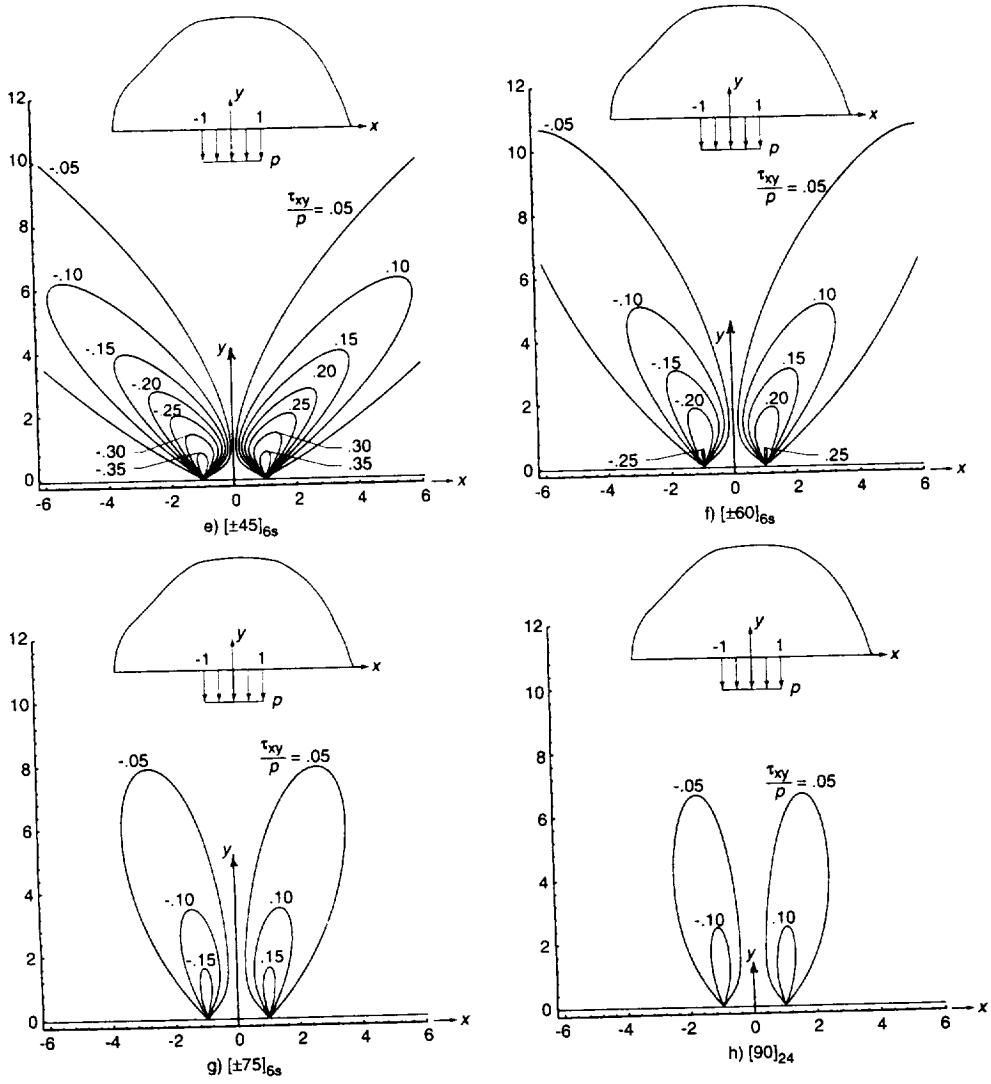

Figure 2. *Constant-τ_{xy} plots for eight different laminates. (Continued).*

ranged from 6.05 to 33.7. These 90% decay distances for the half-planes are presented and discussed in more detail in connection with corresponding results for the elastic strips.

Strip widths that ensure 90% decay

A question that arises is whether the relatively convenient solutions for the half-plane can be useful in the design of similarly loaded strips. A partial answer might be obtained by finding whether there is correlation between the 90% decay distances for the half-planes, y_d, and the minimum strip width required to ensure 90% decay of σ_y across the strip. To this end, the formulas for $\sigma_y(x, h)$ given by Eqs. (24), (31), (37), (52), (59), and (66) were used to find h_d, the minimum value of h for which $\sigma_y(x, h)/p \leq 0.1$ for all x. The process, which involved calculating $\sigma_y(x, h)$ in each laminate for numerous values of h, yielded

Table 2
Comparisons of y_d with minimum strip widths that ensure 90% decay of σ_y

Laminate	y_d, Half-Plane	h_d, Strip A	h_d, Strip B
$[0]_{24}$	9.91	15.0	14.6
$[\pm5]_{6S}$	9.39	14.1	13.6
$[\pm10]_{6S}$	8.35	12.4	11.6
$[\pm15]_{6S}$	7.39	10.7	9.54
$[\pm20]_{6S}$	6.66	9.42	7.74
$[\pm25]_{6S}$	6.18	8.48	6.37
$[\pm30]_{6S}$	6.05	8.21	6.49
$[\pm35]_{6S}$	6.51	8.98	7.43
$[\pm40]_{6S}$	7.30	10.2	8.70
$[\pm45]_{6S}$	8.25	11.6	9.96
$[\pm50]_{6S}$	9.27	13.0	11.1
$[\pm55]_{6S}$	10.4	14.4	11.9
$[\pm60]_{6S}$	12.0	16.2	12.8
$[\pm65]_{6S}$	14.8	20.3	15.2
$[\pm70]_{6S}$	18.4	26.0	21.4
$[\pm75]_{6S}$	22.6	32.7	29.1
$[\pm80]_{6S}$	27.2	40.3	37.8
$[\pm85]_{6S}$	31.5	47.4	45.7
$[90]_{24}$	33.7	50.9	49.5
Isotropic	12.7	18.3	16.2

the values listed in Table 2, which also contains the values of y_d for the corresponding half-planes.

As was the case with some of the type III half-planes, the normal stress $\sigma_y(x, h_d)$ on the supported edge of some type III strips has a relative minimum on its axis of symmetry, which is the y axis. An obvious conclusion from Table 2 is that, for either strip problem, the values of h_d, the minimum strip width required to ensure 90% decay of σ_y, are greater than the corresponding values of y_d, the 90% decay distance in the half-plane. For the strip with the partially fixed edge (problem A), the ratio h_d/y_d varies only moderately among the laminates, from a low of 1.35 for the $[\pm60]_{6S}$ laminate to a high of 1.51 for the $[0]_{24}$ and $[90]_{24}$ laminates. Thus, the use of a single h_d/y_d ratio of about 1.5 for the purpose of designing a specially orthotropic strip on the basis of the half-plane solution appears reasonable.

For the strip with the fixed edge (problem B), however, the range of h_d/y_d is considerably broader, from a low of 1.03 for the $[\pm25]_{6S}$ laminate to a high of 1.47 for the $[0]_{24}$ and $[90]_{24}$ laminates, with most values of h_d/y_d falling below 1.30. Thus, a single value for h_d/y_d of about 1.5 would again serve as an effective upper bound on the panel width required to ensure 90% decay of σ_y. However, because of the larger spread in h_d/y_d, this approach could, for some laminates, lead to wider than necessary strips. Also, in the case of the fixed-edge strip, Table 2 indicates a strong interaction between the intermediate-ply angles and the restraint against tangential displacement along the supported edge, which can result in substantial shear stresses there.

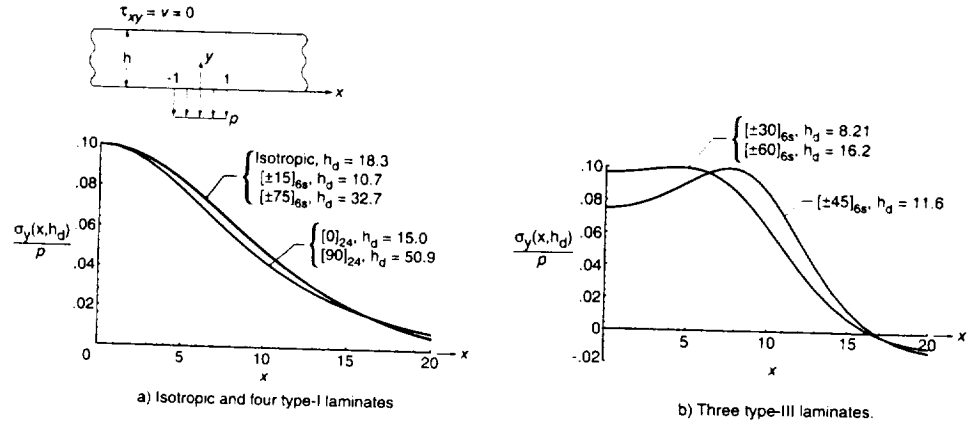

Figure 3. *Graphs of* $\sigma_y(x, h_d)/p$ *for eight laminates (problem A).*

Normal stress on the supported edge

To illustrate the variety of normal stress distributions that occur along the supported edge in response to the localized uniform loading on the opposite edge, $\sigma_y(x, h_d)/p$ is plotted as a function of x in Figure 3 for problem A (partially fixed edge) and in Figure 4 for problem B (fixed edge), for the same eight laminates featured earlier. It is worth noting that identity holds between the graphs of $\sigma_y(x, h_d)/p$ for the following laminate pairs: $[0]_{24}$ and $[90]_{24}$, $[\pm 15]_{6S}$ and $[\pm 75]_{6S}$, and $[\pm 30]_{6S}$ and $[\pm 60]_{6S}$. These identities result from a reciprocal relationship that exists between characteristic values of these pair members because one pair member is the 90° rotation of the other. Note, however, that although the graphs of σ_y on the supported edge of these reciprocal pairs are identical (except for possible minuscule differences due to numerical roundoff), they apply to very different strip widths. Incidentally, the reason for the rather remarkable near-identity in both problems between the graphs of $\sigma_y(x, h_d)/p$ for the isotropic material and for the reciprocal pair $[\pm 15]_{6S}$ and $[\pm 75]_{6S}$ is not apparent to the author.

Figures 3*a* and 4*a* show that graphs of $\sigma_y(x, h_d)/p$ for the isotropic and type I materials differ little, either qualitatively or quantitatively, between problem A and problem B. Figures 3*b* and 4*b* show that graphs of $\sigma_y(x, h_d)/p$ for the type III materials are also qualitatively similar in problems A and B; however, their relative minima on their line of symmetry are

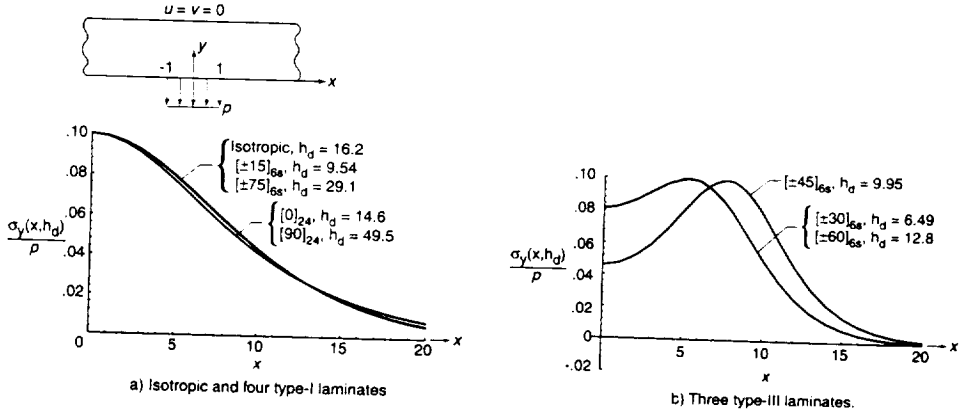

Figure 4. *Graphs of* $\sigma_y(x, h_d)/p$ *for eight laminates (problem B).*

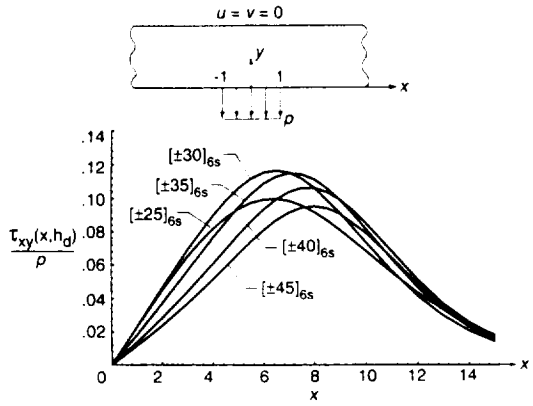

Figure 5. *Graphs of* $\tau_{xy}(x, h_d)/p$ *for five type III laminates.*

more pronounced in problem B, due primarily to the tangential restraint along the edge $y = h_d$. In any event, if a design requirement is at least 90% decay of σ_y across the strip, then for a large number of angle-ply laminates, Table 2 identifies the minimum width needed to satisfy that requirement.

In the case of problem B, however, there is the possibility of significant shear stresses on the fixed edge $y = h_d$. With that possibility in mind, shear stresses along $y = h_d$ were calculated using Eqs. (53), (60), and (67) for type I, type III, and isotropic material, respectively. Significant shear stresses (defined here as satisfying $\tau_{xy}/p \geq 0.1$) on the edge $y = h_d$ were not found in any of the isotropic or type I materials studied. In the type III materials, however, shear stresses that meet the significance criterion were present in the following five laminates: $[\pm 25]_{6S}$, $[\pm 30]_{6S}$, $[\pm 35]_{6S}$, $[\pm 40]_{6S}$, and $[\pm 45]_{6S}$. Plots of $\tau_{xy}(x, h_d)/p$ for these five laminates are shown in Figure 5. By a slight margin, maximum shear stresses on the supported edge are greatest in the $[\pm 30]_{6S}$ and $[\pm 35]_{6S}$ laminates. If shear stresses of this magnitude are of little concern, then the list of h_d values given in Table 2 should suffice as minimum panel widths for design purposes. On the other hand, if these shear stresses are unacceptably large, then Eq. (60) can be used along with appropriate numerical integration tools to determine new, greater panel widths that ensure sufficient decay of both σ_y and τ_{xy}. In the case of the $[\pm 30]_{6S}$ laminate, for example, this augmented criterion would require that the minimum strip width be increased from 6.49 to 7.61.

In the case of problem B, an additional potential complication exists. As a result of the fixed boundary condition, the relation $\sigma_x = \eta_{xy}\sigma_y$ holds everywhere along the edge $y = h$, so that in the small group of laminates for which $\eta_{xy} > 1$ (see Table 1), it follows that $\sigma_x > \sigma_y$ there. Thus, if the 90% decay criterion were to be applied to σ_x as well as to σ_y, then for $\eta_{xy} > 1$ the condition $\sigma_y(x, h_d)/p \leq 0.1$ would have to be replaced by the condition $\eta_{xy}\sigma_y(x, h_d)/p \leq 0.1$, which would result in greater minimum strip widths for a few laminates.

A trend that might, upon first consideration, appear to be counterintuitive can be seen in Table 2. Note that for every laminate the strip width that ensures 90% decay of $\sigma_y(x, h_d)/p$ is greater in problem A (partially clamped edge) than in problem B (clamped edge). This condition is equivalent to the following: for identical laminates of equal strip width, the normal boundary stress that reacts the applied edge loading, i.e., $\sigma_y(x, h)$, has a greater maximum value on the partially fixed edge than on the "stiffer" fully fixed edge. Such a trend runs counter to the popular adage that stiffer boundaries, by offering greater resistance, incur

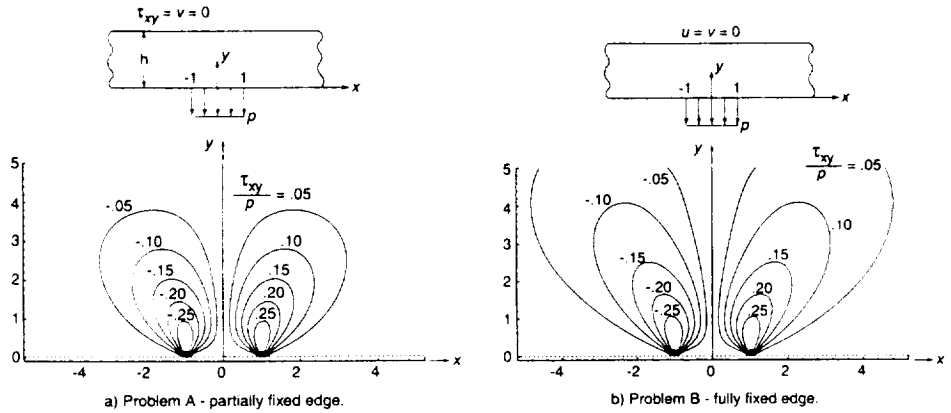

Figure 6. *Shear stress contour plots for the isotropic cases of problems A and B with* $\mathrm{h} = 5$.

greater stress. This apparent anomaly can be resolved by referring to Figures 6*a* and 6*b*, which contain shear stress contour plots for the isotropic cases of problems A and B, respectively, with normalized strip width arbitrarily taken as 5. (The same point can also be illustrated with any of the other laminates and any small-to-moderate strip width.) Note the considerably greater extent of the shear stress field in problem B, as well as the nonzero shear stress distribution on the fixed edge in problem B. At all points on the partially fixed edge of problem A, of course, shear stress is required to be zero. In effect, the restraint against tangential displacement along the fixed edge gives rise to the more extensive shear stress field by which the broader diffusion of the applied normal load is accomplished. A consequence of this broader diffusion of σ_y is lower maximum normal stress on the supported edge. In other words, by promoting greater diffusion of σ_y, the fixed boundary can be said to react the applied load more efficiently than does the partially fixed boundary.

Concluding Remarks

Solutions in the form of improper integrals have been presented for the stresses in a specially orthotropic infinite strip with one edge partially fixed or completely fixed while the other edge is subjected to localized uniform normal loading. In addition, closed-form solutions for the stresses in a similarly loaded specially orthotropic half-plane are obtained. The results are used to generate illustrative contour plots of the direct stress and the shear stress in various half-planes, and to determine minimum strip widths required to ensure 90% decay of stress across the strip.

While the graphical and tabular results presented are for specific laminated composite materials, the formulas for the solutions can be used to calculate the stresses in any similarly loaded specially orthotropic laminated strip or half-plane whenever its elastic constants are known.

References

[1] C. O. Horgan, Recent Developments Concerning Saint-Venant's Principle: A Second Update, *Appl. Mech. Rev.*, vol. 49, pp. S101–S111, 1996.

[2] K. L. Miller and C. O. Horgan, Saint-Venant End Effects for Plane Deformations of Elastic Composites, *Mech. Composite Mater. Struct.*, vol. 2, pp. 203–214, 1995.

[3] W. B. Fichter, Stress Decay in an Orthotropic Half-Plane under Local Self-Equilibrated Edge Loading, *Mech. Composite Mater. Struct.*, vol. 5, pp. 355–370, 1998.

[4] I. S. Gradshteyn and I. M. Ryzhik, *Table of Integrals, Series and Products*, edited by Alan Jeffery, chap. 3, Academic Press, New York, 1980.
[5] N. I. Muskhelishvili, *Some Basic Problems of the Mathematical Theory of Elasticity*, 2d English ed., pp. 395–398, P. Noordhoff Ltd., Groningen, The Netherlands, 1963.
[6] S. Wolfram, *Mathematica—A System for Doing Mathematics by Computer*, 2d ed., Addison-Wesley, Boston, 1991.

APPENDIX: SOLUTIONS FOR ISOTROPIC STRIP PROBLEMS

The method of solution for the isotropic strip problems is identical to that for the orthotropic strip problems; however, in the isotropic case the algebra is somewhat simpler. For isotropic material, Eqs. (1) become

$$\varepsilon_x = u_{,x} = \frac{\sigma_x}{E} - \eta\frac{\sigma_y}{E} \qquad \varepsilon_y = \frac{\sigma_y}{E} - \eta\frac{\sigma_x}{E} \qquad \gamma_{xy} = u_{,y} + \eta_{,x} = \frac{\tau_{xy}}{G} \tag{A1}$$

Equations (2) still give the stresses in terms of the Airy stress function; however, Eq. (3) simplifies to

$$\varphi_{,xxxx} + 2\varphi_{,xxyy} + \varphi_{,yyyy} = 0 \tag{A2}$$

Fourier transforms [see Eqs. (8) and (9)] are again employed. Equation (10) becomes

$$\begin{aligned} &\sigma_{xC} = \varphi_{C,yy} \qquad \sigma_{yC} = -\lambda^2\varphi_C \qquad \tau_{xyS} = \lambda\varphi_{C,y} \\ &u_S = (1/\lambda E)(\varphi_{C,yy} + \eta\lambda^2\varphi_C) \qquad v_C = (1/\lambda^2 E)(\varphi_{C,yyy} - (2+\eta)\lambda^2\varphi_{C,y}) \end{aligned} \tag{A3}$$

and transformation of Eq. (A2) gives

$$\varphi_{C,yyyy} - 2\lambda^2\varphi_{C,yy} + \lambda^4\varphi_C = 0 \tag{A4}$$

For both strip problems, the transformed stress function has the form

$$\varphi_C(\lambda, y) = [A(\lambda) + yB(\lambda)]\cosh\lambda y + [C(\lambda) + yD(\lambda)]\sinh\lambda y \tag{A5}$$

Problem A: Partially fixed upper edge

The transformed boundary conditions are given by Eqs. (12)–(15). Substitution of Eq. (A5) into the transformed boundary conditions leads to four simultaneous equations which have the solution

$$\begin{aligned} A &= -f(\lambda) \\ B &= -2\lambda^2 f(\lambda)\sinh^2\lambda h/\Delta \\ C &= 2\lambda f(\lambda)\sinh^2\lambda h/\Delta \\ D &= 2\lambda^2 f(\lambda)\sinh\lambda h\cosh\lambda h/\Delta \end{aligned} \tag{A6}$$

where

$$\Delta = \lambda(\sinh 2\lambda h + 2\lambda h)$$

Substitution of Eq. (A6) into Eq. (A5), followed by use of the first three of Eq. (10) and Fourier inversion, leads to the stress formulas given by Eqs. (32)–(37).

Problem B: Fixed upper edge

The transformed boundary conditions are given by Eqs. (52)–(55). Substitution of Eq. (A5) into Eqs. (52)–(55) leads to simultaneous equations which have the solution

$$\begin{aligned} A &= -f(\lambda) \\ B &= -\lambda f(\lambda)[(3-\eta)\sinh\lambda h\cosh\lambda h - (1+\eta)\lambda h]/D \\ C &= \lambda f(\lambda)[(3-\eta)\sinh\lambda h\cosh\lambda h - (1+\eta)\lambda h]/D \\ D &= \lambda f(\lambda)[(3-\eta)\sinh^2\lambda h + 2]/D \end{aligned} \tag{A7}$$

where

$$D = l[(3-n)\sinh^2 lh + (1+n)l^2h^2 + 4/(1+n)]$$

Substitution of Eq. (A7) into Eq. (A5), use of the first three of Eq. (10) and Fourier inversion yield the stress formulas given by Eqs. (61)–(67).